Agricultural and Forest Meteorology 307 (2021) 108517

Contents lists available at ScienceDirect

Agricultural and Forest Meteorology

journal homepage: www.elsevier.com/locate/agrformet

Towards robust on-site ammonia emission measuring techniques based on inverse dispersion modeling

Eva Herrero [a,*], Alberto Sanz-Cobena [b], Viviana Guido [c,1], Mónica Guillén [a], Arturo Dauden [a], Rocío Rodríguez [b], Giorgio Provolo [c], Dolores Quílez [a]

[a] Unidad de Suelos y Riegos, Centro de Investigación y Tecnología Agroalimentaria de Aragón (CITA). Avda. Montañana 930, Zaragoza 50059, Spain
[b] Research Center for the Management of Environmental and Agricultural Risks (CEIGRAM), Universidad Politécnica de Madrid, Senda del Rey 13, Madrid 28040, Spain
[c] Department of Agricultural and Environmental Sciences, University of Milan, via Celoria 2, Milan 20133, Italy

ARTICLE INFO

Keywords:
Micrometeorological methods
Mass balance integrated horizontal flux
Ammonia volatilization
Inverse dispersion
Diffusion passive sampler
Semi-arid regions

ABSTRACT

Ammonia is recognized as one of the major atmospheric pollutants affecting air and ecosystem quality. The application of N fertilizers is a major source of NH_3 emissions. It is necessary to develop simple, accurate and low cost measurement techniques to obtain representative data for a wide range of regions and agricultural practices. This information would improve national inventories and support decision-making processes regarding strategies for NH_3 emission abatement. Measurement techniques can be complex, adjusted to specific conditions, labor-intensive and costly. This work analyses different methods aimed at reaching a balance between the accuracy and precision required for measurements and their complexity. Three techniques were tested under: semiopen passive chambers (SOCs) and an inverse dispersion model (IDM) combined with two different NH_3 air concentration measuring techniques: ALPHA® passive samplers and acid bubblers. Different setups were evaluated testing different heights over the emitting surface. These techniques were assessed using micrometeorological mass balance integrated horizontal flux (IHF) with passive flux samplers as a reference method. The SOC results showed a close linear relationship with the IHF results (R^2=0.784, $p<0.01$), although emissions after 16 days were 10.6% higher. The bLS IDM with acid bubblers showed promising results, although they were labor-demanding and required a power supply. The IDM with ALPHA® samplers placed at a 1.25-m height was demonstrated to embrace precision and close agreement with the IHF observations in our experimental conditions (R^2=0.768, $p<0.01$; no difference from line 1:1; mean bias: 0.041 kg N $ha^{-1}h^{-1}$ and rRMSE: 46.1%). However, these data require special attention for periods of drastically changing weather, when the NH_3 fluxes determined with air concentration samplers moved away from the overall emission pattern. Longer sampling intervals and the assumption of neutral atmospheric conditions in IDM may decrease costs, simplify the procedure and provide a cost-efficient alternative to the IHF method.

1. Introduction

Ammonia (NH_3) emissions cause environmental damage through air pollution and natural ecosystem degradation and contribute significantly to the formation of fine particulate matter, which is considered a major public health concern (European Environmental Agency, 2019; WHO, 2019). Fertilizing activities and animal husbandry are responsible for 80% of the global NH_3 emissions caused by human activity (UNEP, 2019). Moreover, these emissions represent a loss of fertilizer nitrogen (N); this loss impairs N fertilization efficiency and the economic balance of farms.

There is high uncertainty in quantifying NH_3 emissions from agricultural activities, as wide varieties largely influence these emissions in local practices and pedoclimatic conditions that act as drivers of N dynamics. National inventory methodologies and official reports often use databases and default emission factors supported by experimental information and lack field observations in semi-arid regions (Flesch et al., 2014; Misselbrook et al., 2005; Ni et al., 2015; Pedersen et al., 2020). The construction of robust and reliable databases relies on precise and simple on-site monitoring techniques that are sensitive to local

* Corresponding author.
E-mail address: eherrero@cita-aragon.es (E. Herrero).
[1] Present address: Associazione Regionale Allevatori Lombardia. Via Kennedy 30, 26013 Crema, Italy.

https://doi.org/10.1016/j.agrformet.2021.108517
Received 3 December 2020; Received in revised form 10 June 2021; Accepted 12 June 2021
Available online 30 June 2021

conditions. The standardization of low-resource-demanding methodologies that are easy to replicate can contribute to the acquisition of valuable NH_3 emission data as a basis for the proposal of cost-effective and region-based NH_3-mitigating agricultural strategies (Sanz-Cobena et al., 2014). It is necessary to evaluate and tune the NH_3 measuring techniques available in the semi-arid climatic conditions and discern their potential uses to reach this objective. The importance of assessing measurement techniques in a regional-based approach relies on the fact that the effectiveness of both measurement devices (e.g. acid bubblers) and calculation methods could be affected by specific meteorological conditions, e.g., passive badge-type samplers can be sensitive to wind conditions (Tang et al., 2001); in semiopen passive chambers, trapping efficiency requires experimental cross-calibration against recognized reference methods under local weather and agronomic patterns (Martins et al., 2021) and high atmospheric stability strongly affects assumptions made in estimating ammonia fluxes by dispersion modeling (Theobald et al., 2015).

Enclosure methods such as closed and semiopen passive chambers or wind tunnels are frequently used in small plots on bare or prairie soils by the scientific community (Sanz-Cobena et al., 2011). Nevertheless, these methods have less spatial representativeness and could affect environmental conditions during the measurement period, including key parameters affecting NH_3 emissions such as wind speed or temperature. Consequently, the absolute emission rates obtained through these methods may differ considerably from the real conditions (Misselbrook et al., 2005; Ni et al., 2015; Scotto di Perta et al., 2019). Semiopen passive systems such as the method described in Araújo et al. (2009) are less intrusive and may represent a practical, low-cost approach for comparing different treatments simultaneously under the same conditions (Jantalia et al., 2012). Wind tunnels could also be a good alternative, for comparative purposes in small plots but they require a power supply, present higher costs, and are labor demanding (Pedersen et al., 2020; Shah et al., 2006).

Micrometeorological methods, such as the integrated horizontal flux (IHF) method, the theoretical profile shape method (Z_{inst}), or backward Lagrangian stochastic methods used in the inverse dispersion model (bLS IDM) are able to determine NH_3 emissions in a nonintrusive manner; this ability causes these methods to be better options for determining absolute NH_3 fluxes from medium and large emitting sources than the more intrusive methods listed above (Misselbrook et al., 2005). The IHF method, originally presented by Denmead (1983), is considered a reference method and has been validated, in combination with passive flux samplers (Leuning et al., 1985), by several research groups worldwide (Laubach et al., 2012; Misselbrook et al., 2005; Sanz-Cobena et al., 2008; Sintermann et al., 2012; Sommer et al., 2005; Yang et al., 2019). However, its efficacy may be constrained in irregularly shaped plots or large emitting areas that may require high measuring heights that considerably complicate monitoring work (i.e., $>$ 1 ha) (Sanz et al., 2010). In addition, this method is time-consuming and resource-demanding in the laboratory and during fieldwork, and its transferability to larger productive fields and specific real agricultural scenarios is limited. The Z_{inst} method infers the average surface flux density for a constant surface geometry using a time series of horizontal flux density measurements at a single height (Wilson et al., 1982). This method considerably reduces setup costs and laboratory work. This is supported by theoretical and empirical evidence that under certain conditions and sizes of homogeneous emitting surfaces, there is a height interval in which the air concentration is insensitive to the air layer stability regime (Denmead, 1983; Wilson et al., 1983, 1982). Geometric and size plot conditions constrain the use of the Zinst method.

Alternatively, bLS IDM shares similar operational requirements to Z_{inst} but benefits from fewer restrictions regarding the shape or dimensions of the emitting source. In return, bLS IDM faces the challenge of using air NH_3 concentration samplers with short exposure periods that ensure homogeneous atmospheric stability. Optical remote sensing systems (i.e., open path lasers or cavity ringdown analyzers) provide promising results based on accurate real-time observations (Insausti et al., 2020; Ni et al., 2015; Shonkwiler and Ham, 2018; Wilson et al., 2012). However, these systems require substantially higher investments, power supplies and highly skilled knowledge and training for their operation, which hinders their replication and transferability. Passive flux samplers have been used extensively in the literature (Laubach et al., 2012; Ni et al., 2015; Sanz et al., 2010; Sommer et al., 2005; Turner et al., 2010), even though their use can be labor-demanding in the laboratory and their measurements are sensitive to turbulent backflow or bad alignment with upwind direction and stalling problems under low-wind conditions (Leuning et al. 1985; Laubach et al., 2012). Additionally, bLS IDM software (i.e., WindTrax, Thunderbirdscientific) requires separate inputs of wind speed records and time-average NH_3 air concentration. Diffuse samplers are low-cost alternatives that are simple and easy to handle. Although they were initially designed for measuring average concentrations over long exposure intervals, badge-type samplers, such as ALPHA® (Adapted Low-cost Passive High Absorption) samplers (APSs), have faster sampling rates, although they are more sensitive to wind speed than other types of samplers (Tang et al., 2001). Nevertheless, some studies demonstrated that APSs combined with the bLS IDM presented acceptable precision and accuracy over short intervals (from 1 day to 1 week) and at high concentrations (up to 100 μg m^{-3}) without saturation (Puchalski et al., 2011). Sommer et al. (2005) suggested that, based on the Z_{inst} method principles and using the appropriate sampling height, the bLS IDM sensitivity to atmospheric stability can be minimized. Thus, considering neutral atmospheric conditions for periods longer than a few hours may not hinder NH_3 emission rate determinations, even despite the effects of day and night on atmospheric stability. The monitoring height is a determining factor, which may also be related to emitting surface size when considering atmospheric stability throughout long periods as neutral conditions (Loubet et al., 2010; Sommer et al., 2005). This study tested different sampler displacements in 25 m-radius plots to determine the measuring height at which daily variations in atmospheric stability had less effect on the results and allowed us to obtain emissions quantitatively closer to those obtained with the IHF reference method. Some authors have compared the performance of bLS IDM against the IHF using passive flux samplers or acid bubblers (Laubach et al., 2012; Sommer et al., 2005; Turner et al., 2010; Häni et al., 2016). Other studies have also tested different height displacements for samplers in inverse dispersion modeling (Häni et al., 2016; Loubet et al., 2018; Sommer et al., 2005). However, no information has been found about simultaneous method comparison using the IHF method as a reference technique and comprising the wide variety of methods included in this study. SOCs and bLS IDM, under the assumption of neutral conditions, test different measuring heights with ALPHA samplers and acid bubblers.

In this context, this study hypothesizes that alternative simplified easy-to-replicate methods driven by readily measured parameters can estimate NH_3 fluxes with a suitable degree of accuracy based on simple source samplers while reducing labor demands and material costs. The work addresses two main objectives. First, three alternative approaches for on-site determination of NH_3 emissions in semi-arid agricultural systems were compared with the full-profile mass balance IHF method coupled with passive flux samplers: 1) semiopen passive chambers (SOCs); 2) the bLS IDM combined with APSs, and 3) the bLS IDM combined with acid bubblers (ABs). Second, the effect of sampler heights, four with APSs and two with ABs, on the determination of NH_3 emissions with bLS IDM was assessed.

2. Materials and methods

2.1. Experimental site

The experiment was conducted in 2019 from October 28th to November 13th in a 1.30-ha field located in the middle Ebro valley (Zaragoza, Spain: 41°42'50.1 "N, 0°49'32.8 "W) on bare soil. The

topsoil (0-30 cm) has a loamy texture (48.8% sand, 35.4% silt, 15.8% clay) and a pH of 8.4. The area is characterized by a flat landscape and semi-arid climate (annual average temperature of 14.6°C, 324 mm annual precipitation and 1239 mm annual reference evapotranspiration (ETo) (period 2003-2020). There were no physical barriers 200 m beyond the field's boundaries, and the agricultural fields within 500 m remained inactive during the experiment.

2.2. Experimental design

The experimental layout comprised two 25-m radius circular plots (P1 and P2) with a distance between their borders of approximately 50 m. A central mast was installed in each plot, and three background sites (BG1, BG2, and BG3) were also equipped to detect any influence of an external NH_3 source coming from any of the prevailing wind directions in the area (Fig. 1).

Urea was evenly applied to the land surface by hand at a rate of 184 kg N ha^{-1} at 11:00 AM on October 28th. Emission monitoring started 2 h later and lasted 16 days. Sampling was performed daily during the first four days and less frequently afterward at a rate of 1 sample every 2-3 days.

Four different devices were used to sample ammonia in the air (Table 1): i) passive flux samplers (PFSs) were used for the IHF method, ii) semiopen passive chambers (SOCs), iii) APSs with the IDM, and iv) acid bubblers (ABs) with the IDM (Fig. 1).

Passive flux samplers (Leuning et al., 1985) were installed in the central masts of P1 and P2 at 0.25-, 0.65-, 1.25-, 2.05- and 3.05-m heights over the soil surfaces. The masts installed at BG1 and BG2 (Fig. 1) were equipped with 3 PFSs at heights of 0.25 m, 1.25 m, and 3.05 m, following a setup and procedure previously used under semi-arid conditions and detailed in Sanz-Cobena et al. (2008). The holders allowed the PFSs to rotate on the vertical axis, ensuring a permanent orientation towards the main wind direction. The internal surfaces of the PFSs were coated with 30 ml of oxalic acid and acetone solution and sealed for transport to the field. A blank PFS was brought into the field next to the others during every replacement as a sampler contamination control. After every PFS replacement, the samplers were immediately sealed, transported to the laboratory, and flushed with 40 ml of deionized water for ammonium (NH_4^+) concentration determination (Section 2.5).

Table 1
Samplers and NH_3 emission measuring methods.

NH_3 samplers
Passive flux samplers (PFSs)
ALPHA® passive samplers (APSs)
Acid bubblers (ABs)
Semiopen passive chambers (SOCs)
NH_3 emission measuring methods
Mass balance Integrated Horizontal Flux (IHF)
Backward Lagrangian stochastic inverse dispersion model (bLS IDM)
Semiopen passive chamber mass balance (SOC mass balance)

The semiopen passive chambers were built according to the methods outlined in Araújo et al. (2009) and were placed along one radius of P1 and P2, with six in each plot separated by 4 m and 1 cm above the soil surface. A background set was installed in BG3 with 6 SOCs distributed in the same way over bare soil that was not fertilized (Fig. 1). The absorbent system's foam strip was dampened in an H_2SO_4 acid solution (1 mol H_2SO_4 dm^{-3} (10%) + glycerine, 2% v/v) and placed in a 50-mL plastic jar filled with the same solution to maintain the moisture of the foam strip. After every sampling interval, the foam was soaked in 50 ml of 2 M KCl and taken to the laboratory, where the solution was gauged up to 250 ml with 2 M KCl for NH_4^+ concentration determination (Section 2.5).

The APSs, developed by the Centre of Ecology & Hydrology (UK) and detailed Tang et al. (2001), were used following the sampling procedures described in Tang et al. (2017). The samplers were installed in the central masts of P1 and P2 at heights of 0.65, 1.25, 2.05, and 3.05 m and in BG1 and BG2 at heights of 0.25, 1.25, and 3.05 m. At every position, triplicate samplers were used. A blank sampler was always brought to the field next to the other samplers as a contamination control of the samplers during the replacement and transport operations. The cellulose fiber filters were coated with a citric acid and methanol solution (13% m/v) before their exposure. After exposure, the NH_4^+ trapped in the coated filters was extracted with 3 ml of deionized water for NH_4^+

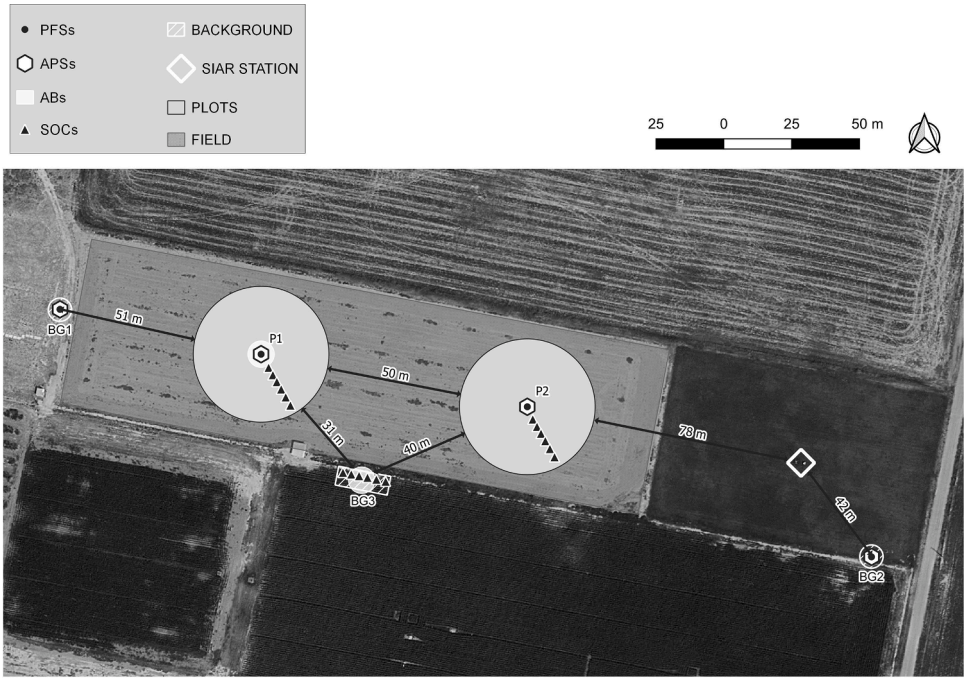

Fig. 1. Layout of the experimental setup.

concentration determination (Section 2.5). Only APS concentrations above twice the average NH_4^+ concentration determined in every 3-sample batch were discarded.

The ABs were used following the setup described in Perazzolo et al. (2015). P1 was equipped with 2 AB collecting systems sampling air at 2.05- and 1.25-m heights above the ground. Each had a single airflow intake open to the free air and fixed in the center mast. An average 6.5 L min^{-1} airflow, controlled with a gas measuring counter and an analog flowmeter, was forced with a vacuum pump (EVO30 series, Oead) through Teflon® tubes (6 mm inner diameter) into 2 Drechsel bottles connected in line and containing 200 ml of 1% boric acid each. Two background ABs were set in the BG3 mast at the same heights, following an identical scheme used for P1. The acid solutions in the Drechsel bottles were replaced synchronously with the PFSs, SOCs, and APSs sampling intervals except on 2 occasions. The collection systems were removed from the field twice during the experiment (between 94 and 167 h and between 261 and 333 h) when the field was not under surveillance to avoid damage to the glass material used for monitoring. The 1% boric acid solution in the collection vessels was immediately transported to the laboratory for NH_4^+ concentration determination (Section 2.5).

All the sampling devices (PFSs, SOCs, APSs, and ABs) were replaced concurrently and spanned identical time intervals (Supplementary material, picture compilation).

2.3. Meteorological measurements

Meteorological data were recorded from the SIAR network (agroclimatic information system for irrigation), station Z-11 Montañana, http://eportal.mapa.gob.es/websiar/Ficha.aspx?IdProvincia=50&IdEstacion=11). More information is detailed in Image S1 (Supplementary material).

Averaged 30-min wind speed (m s^{-1}), wind direction (°; moving clockwise, north=0°), temperature (°C), relative humidity (%), and precipitation (mm) data were obtained from a weather station placed 50 m E-SE from the experimental field.

2.4. NH_3 emission fluxes

The net NH_3 flux (F, μg N m^{-2} s^{-1}) in each sampling period was estimated using i) the IHF mass balance coupled with PFSs, ii) the SOC mass balance, and iii) the bLS IDM combined with air NH_3 concentrations monitored with APSs and ABs (Table 1).

The IHF micrometeorological method relies on mass balance by measuring horizontal NH_3 flow rates at different heights from an emitting surface at a known distance downwind. F was derived using Eq. (1) from the time-averaged horizontal flux, $\overline{uc}$, measured at 3 heights upwind, at the background masts, (uw) and 5 levels downwind (dw), at the center of the plots, according to Eq. (2) (Misselbrook et al., 2005):

$$F = \frac{1}{x}\left[\int_0^z (uc)_{dw}dz - \int_0^z (uc)_{uw}dz\right] \quad (1)$$

$$\overline{uc} = \frac{M_{N-NH_4^+}}{A\ t} \quad (2)$$

where M is the mass of N-NH_3 (μg) trapped during the sampler exposure period, A is the effective cross-sectional area of the PFS (m^2), t is the time of exposure of every PFS (s) and z is the top position in the mast occupied by a sampler (m). The mean fetch length (x) was the radius of the plots, 25 m. The net integrated horizontal flux was obtained by adding horizontal fluxes between every two consecutive measurement heights. The horizontal flux between two consecutive heights was obtained by multiplying the height difference by the average of the horizontal flux measured at both heights. The net horizontal flux at 0 m height is assumed to be 0. Horizontal diffusion is neglected, considering that it is expected to be small compared to horizontal convection flux (Denmead, 1983; Leuning et al., 1985).

The SOC mass balance deducts F considering the mass of N-NH_4^+ absorbed in the foam, the exposure time ($M_{N\text{-}NH4}^+$, μg N s^{-1}), the monitored surface (0.007854 m^2), and an absorption efficiency factor (E_{SOC}) of 24.6% obtained by Mateo-Marín et al. (2021), also in line with Martins et al. (2021) (24% when the chamber is placed 10 mm above the soil surface), using Eq. (3).

$$F = \frac{M_{N-NH_4^+} \times E_{SOC}}{0.007854} \quad (3)$$

The bLS dispersion model is described in detail by Flesch et al. (2004). The inverse dispersion model infers F from a known emitting surface using upwind and downwind air NH_3 concentrations measured at a single height (C_{NH_3}, μg m^{-3}), surface roughness length (z_o, cm), and atmospheric stability and considering wind data (Loubet et al., 2010). The atmospheric dispersion modeling software used for this work was WindTrax v.2.0.8.9 (Thunder Beach Scientific, Halifax, Nova Scotia, Canada).

Our experimental design complies with the requirements for ensuring spatial homogeneity of the emitting surface when the fetches are larger than 20 m (Carozzi et al., 2013a; Loubet et al., 2010).

One of the main limiting factors of the bLS IDM is the necessity of using short sampling periods that ensure homogeneous atmospheric stability. This work assumed the recommendations of Sommer et al. (2005), which were also discussed and adopted in previous research (e.g., Carozzi et al., 2013b; Ni et al., 2015; Sanz et al., 2010), and tested longer intervals (ranging from 24 to 72 h) considering neutral atmospheric stability.

The value of z_o (the height above the soil surface at which the wind speed reaches zero) was considered equal to 1 cm, a default value that corresponds to bare soil with no effects of crop canopy height and density.

The NH_3 emission flux for each measurement period was calculated using 30-min interval WindTrax runs. The average emission flux for every period was obtained by averaging 30-min fluxes. The inputs for each software run were i) average half-hour wind speed (m s^{-1}), ii) average NH_3 air concentration measured in the center mast of the plot during every sampling period, and iii) average NH_3 air concentration measured in one of the background masts (BG1 or BG2), selected half-hourly according to the prevailing upwind direction. The average NH_3 air concentrations (C_{NH_3}, μg m^{-3}) were determined using information from the APSs and ABs. The APSs operate on the principles of the diffusion of gases, as described in Tang et al. (2001), and C_{NH3} was calculated according to the air volume sampled, according to Fick's law (Eq. (4)), using Eq. (5):

$$V = \frac{DA}{L} \times t \quad (4)$$

$$C_{NH_3} = \frac{M_{NH_3}}{V} \quad (5)$$

where M_{NH_3} is the average mass of NH_3 (μg) collected in triplicate samplers at every exposure time, V (m^3) is the volume of air sampled, t is the time of exposure (h), D is the diffusion coefficient of NH_3 (m^2 s^{-1}) at 20°C, A is the cross-sectional area (m^2) of the APS and L is the length (m) of the stationary air layer within each APS. Wind may influence APS performance, entailing the need for the empirical determination of a correction factor for the effective NH_3 uptake rate (Tang et al., 2001). Nevertheless, in this study no correction factor was applied based on the use of long-term sampling periods comprising a wide variety of wind conditions and the search for the simplest possible measuring methods.

The emission flux at every exposure time was estimated for every sampling height; the emission fluxes at 3.05 m and 1.25 m were estimated using background concentrations at the same heights; for 2.05 m

and 0.65 m heights, the emission fluxes were estimated using background concentrations at 1.25 m (the closest background height position). BG2 was used as the background for wind direction records ranging from 30° to 220°; otherwise, BG1 was selected as the background.

In the AB samples, C_{NH_3} was calculated using Eq. (6):

$$C_{N-NH_3} = \frac{M_{N-NH_4^+}}{V} \quad (6)$$

where V is the volume of air (m^3) recorded in an air counter, and $M_{N\text{-}NH4^+}$ is the mass of $N\text{-}NH_4^+$ (μg) trapped in the vessel. The emission fluxes were calculated with WindTrax for the two sampling heights using background concentrations (BG3) obtained at the same heights. The missing flux data in the AB observations (between 94 and 167 h and between 261 and 333 h) were estimated by interpolating the average emission flow rate between the preceding and posterior sampling periods.

2.5. Soil sampling

The soil (0-10 cm depth) was sampled before applying urea (October 28th), and sampling continued every 2-4 days until the end of the experiment. Four composite samples (each made of 3 subsamples) were taken per plot, one in each quarter of the circular surface, with an auger (5-cm diameter). Soil samples were sieved through a 3-mm mesh and transported to the laboratory. Then, the water content was determined by gravimetry (drying at 105°C), and 1:3 soil extracts (10 g fresh soil + 30 ml 2N KCl solution) were prepared for NH_4^+ concentration determination.

2.6. Analytical determinations

The ammonium concentration in the aqueous extracts from the passive flux sampler, semiopen passive chambers, alpha samplers, and soil sampling was determined by colorimetry following the salicylate method with nitroprusside (Searle, 1984) in a segmented flow analyzer (AutoAnalyser3, Bran+Luebbe, Norderstedt, Germany). The mass of ammonium in the extracts was determined by multiplying the NH_4^+ concentration by the extract volume.

2.7. Statistical analysis

The ammonia emission flux obtained with the reference method (IHF) for each sampling interval was compared to the estimates acquired by the other methods at different sampling heights using different statistical tools. The goodness of the model was assessed by different statistical parameters. Linear regression was used to analyze the strength of the relationship between the IHF results and the fluxes determined with other methods. The regression's significance was established by the analysis of variance F-test (p=0.01) and characterized by the coefficient of determination (R^2). The estimation methods can give values highly related to the IHF values but can overestimate or underestimate the reference values; for that reason, the fitted line was compared to the 1:1 line (intercept different than zero and slope different than 1) using a t-test at p=0.01 (Statgraphics Technologies, Inc., USA). In addition, the mean bias (MB, Eq. (7)) was used to measure the average tendency of the estimates to be larger or smaller than the IHF values. The relative root mean square error (rRMSE, Eq. (8)) was used to compare errors between the different models; the lower the rRMSE was, the better the model and the Nash-Sutcliffe efficiency (NSE) was used to determine the relative magnitude of the residual variance compared to the measured data variance (Eq. (9)). The NSE was also calculated in its modified version (E1), with absolute values substituting squared differences, which allows the metric to be less sensitive to outliers (Eq. (10)) (Lorenzo-Gonzalez et al., 2013). The NSE and E1 values range between -∞ and 1; values between 0 and 1 are considered acceptable levels of performance (a value equal to 1 indicates a perfect fit), and negative values indicate unacceptable performances of the estimates.

$$MB = \frac{\sum_{i=1}^{N}\left(F_i^{IHF} - F_i^{est}\right)}{N} \quad (7)$$

$$rRMSE = \frac{\left[\frac{\sum_{i=1}^{N}\left(F_i^{IHF} - F_i^{est}\right)}{N}\right]^{0.5}}{\frac{\sum_{i=1}^{N} F_i^{est}}{N}} \quad (8)$$

$$NSE = 1 - \left[\frac{\sum_{i=1}^{N}\left(F_i^{IHF} - F_i^{est}\right)^2}{\sum_{i=1}^{N}\left(F_i^{IHF} - F_m^{IHF}\right)^2}\right] \quad (9)$$

$$E1 = 1 - \frac{\sum_{i=1}^{N}\left|F_i^{IHF} - F_i^{est}\right|}{\sum_{i=1}^{N}\left|F_i^{IHF} - F_m^{IHF}\right|} \quad (10)$$

In the above equations, F_i^{IHF} is the IHF-obtained NH_3 flux for time interval i; F_i^{est} denotes the NH_3 flux estimate for time interval i; F_m^{IHF} is the average of the IHF-obtained NH_3 fluxes, and N is the number of sampling intervals.

3. Results

3.1. Soil and weather conditions

The average initial soil (0-10 cm) water content before urea spreading was 0.158 g g^{-1} (±0.007 SE) in P1 and 0.153 g g^{-1} (±0.004 SE) in P2. Before fertilization, the soil ammonium concentration was less than 0.1 mg $N\text{-}NH_4^+$ kg^{-1} (0.15 kg $N\text{-}NH_4^+$ ha^{-1}, Supplementary material, Table S1).

The average temperature during the experiment was 12.6°C; the temperature ranged from 1.2°C to 24.2°C. The mean atmospheric thermal tide was 9.7°C between day and night. The first 72 h after urea application (HAUA) was characterized by warm and low-wind average atmospheric conditions (14.8°C and 0.9 m/s, respectively), combined with thick daily foggy episodes in the morning. The relative humidity reached 100% during some hours (Fig. 2); afterward, the wind speed increased, and the average values raised to 2.6 m s^{-1}.

The prevailing wind direction followed the usual wind pattern observed in the Ebro valley (WNW-NW). Approximately 80% of the semihourly wind records came from 220 to 20° with an average wind speed value of 3.1 (±2.1 SD) m s^{-1}, while 20% of the semihourly records ranged from 30 to 220° with an average wind speed of 0.8 (±0.5 SD) m s^{-1}. The background values used in the bLS IDM micrometeorological method were mostly derived from BG1.

There were 3 rainfall events with magnitudes higher than 3 mm. They occurred on November 3rd (139 HAUA) with 3.2 mm rainfall concurrent with a 2-hour windy period that ranged from 6.0 m s^{-1} to 9.6 m s^{-1}, November 8th (266 HAUA) with 4.24 mm rainfall coincident with peaking winds (> 5.1 m s^{-1}) and on the night of November 13th (375 HAUA) with 6.46 mm rainfall and an average wind speed that dropped to 0.65 m s^{-1} (Fig. 2).

3.2. Ammonia daily fluxes

The ammonia flux estimates maintained a similar pattern to the IHF-observed fluxes during the experimental period, reaching a peak of 94 h after urea application with an average IHF value of 0.34 kg $N\text{-}NH_3$ ha^{-1} h^{-1} (±0.02 S.E.) (Fig. 3).

The ammonia fluxes measured with SOCs presented a strong linear relation (R^2=0.784, p<0.01) with the IHF values that did not differ from the 1:1 line (Table 2) and presented the lowest bias and NSE and E1 values closest to 1.

The fluxes derived from APSs at the height of 3.05 m showed a poor relation to the IHF values; these flux estimates obtained the highest

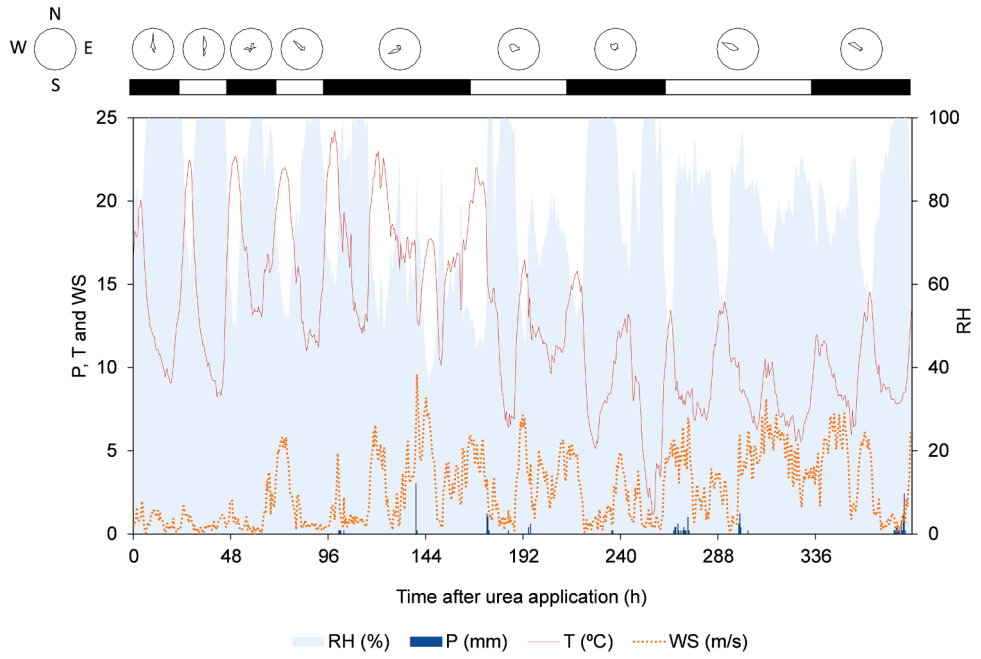

Fig. 2. Precipitation (P), temperature (T), wind speed (WS), wind directions (compass rose on the top) and relative humidity (RH). Semihourly records.

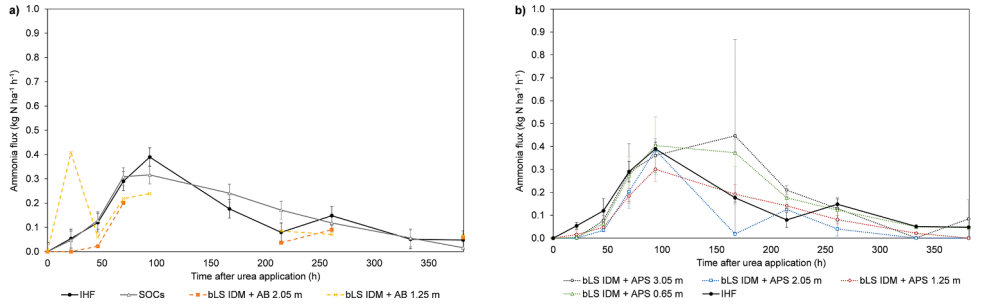

Fig. 3. Average (n=2) IHF-obtained NH_3 emission fluxes and NH_3 emission fluxes determined at the two plots using a) the IHF method, SOCs and ABs at heights of 1.25 and 2.05 m, combined with the IDM, and b) APSs at heights of 0.65, 1.25, 2.05 and 3.05 m, combined with the inverse dispersion model (vertical bars denote the standard errors).

Table 2
Statistics of the comparative analysis of NH_3 fluxes (kg N ha^{-1} h^{-1}) between the reference (IHF) and the determinations obtained using semiopen passive chambers and a backward Lagrangian stochastic inverse dispersion model combined with ALPHA® samplers (APS) at heights of 0.65, 1.25, 2.05 and 3.05 m and with acid bubblers (ABs) at heights of 1.25 and 2.05 m. The coefficient of determination (R^2) intercept (kg N ha^{-1} h^{-1}) and the slope of the linear regression, mean bias (MB, kg N ha^{-1} h^{-1}) root mean square error (rRMSE, %), Nash-Sutcliffe efficiency (NSE), modified efficiency (E1), and number of data pairs (N) are shown in the table.

	Linear Regression			Mean bias	rRMSE	NSE	E1	N
IHF versus	R^2	Intercept	Slope					
APS 0.65	0.667[a]	0.007[b]	1.066[c]	-0.017	59.3	0.631	0.687	18
APS 1.25	0.768[a]	-0.004[b]	0.755	0.041	46.1	0.713	0.670	18
APS 2.05	0.770[a]	-0.054[b]	0.955 [c]	0.061	57.2	0.644	0.670	18
APS 3.05	0.243	0.040[b]	0.910[c]	-0.027	124.9	0.222	0.670	18
AB 1.25	0.046	0.129[b]	0.191 [c]	0.016	108.0	0.254	0.267	7
AB 2.05	0.695	-0.006[b]	0.533 [c]	0.121	62.0	0.725	0.670	6
SOCs	0.784[a]	0.025[b]	0.870 [c]	-0.005	36.7	0.771	0.862	18

[a] Significant regression line ($p < 0.01$).
[b] not significantly different than 0 ($p > 0.01$).
[c] not significantly different than 1 ($p > 0.01$).

rRMSE and the lowest NSE values. Meanwhile, the fluxes derived from APSs at the other heights showed strong relations with the IHF values and good fits to the 1:1 line. However, the APS estimates at 1.25 m showed higher NSE (closer to 1) (Table 2). The coefficient of variation (CV) of every 3-sample batch (without discarding outliers) for each height and period in the sampling masts ranged from 0 to 50%, increasing with sampling height and in sampling intervals with lower N-NH_3 samples (1, 2, 8 and 9). In the BG masts, CV was higher than for the sampling masts (reaching 88%) associated with lower N-NH_3 concentrations. Average CVs were 31.7% at 3.05 m, 20.8% at 2.05 m, 14.5% at 1.25 m, and 14.2% at 0.65 m (Supplementary material, Table S4 and Fig. S1).

The inverse dispersion model combined with ABs presented a nonsignificant linear relation with the IHF values and a distant adjustment to line 1:1 (Fig. 4), with slopes different than 1 (Table 2) and a low NSE value for the 1.25-m height (Table 2). The slope derived from the linear regression analysis at both heights for the ABs led to considerable underestimations of the emissions. The statistical analysis was strongly affected by the low number of observations (7 for the AB at 1.25 m and 6 for the AB at 2.05 m).

3.3. *Cumulative NH_3 emissions*

The average cumulative NH_3 emissions at 214 HAUA (9 days) in the two plots ranged from 18.7 (from the bLS IDM with an AB at 2.05 m) to 59.64 kg N ha^{-1} (the bLS IDM with the APSs at 3.05 m) (Fig. 5). After 9 days (214 HAUA), the average fraction of cumulative losses obtained in the 14 measurements performed (8 in P1 and 6 in P2) reached 80% (±3% SE) of the total emissions achieved at the end of the experiment (381 HAUA) (Supplementary material, Table S2).

The cumulative emissions measured at the end of the experiment with the IHF (i.e., the reference technique in this experiment) reached 50.1 kg N ha^{-1}.

The SOC and bLS IDM methods measured at the height of 1.25 m,

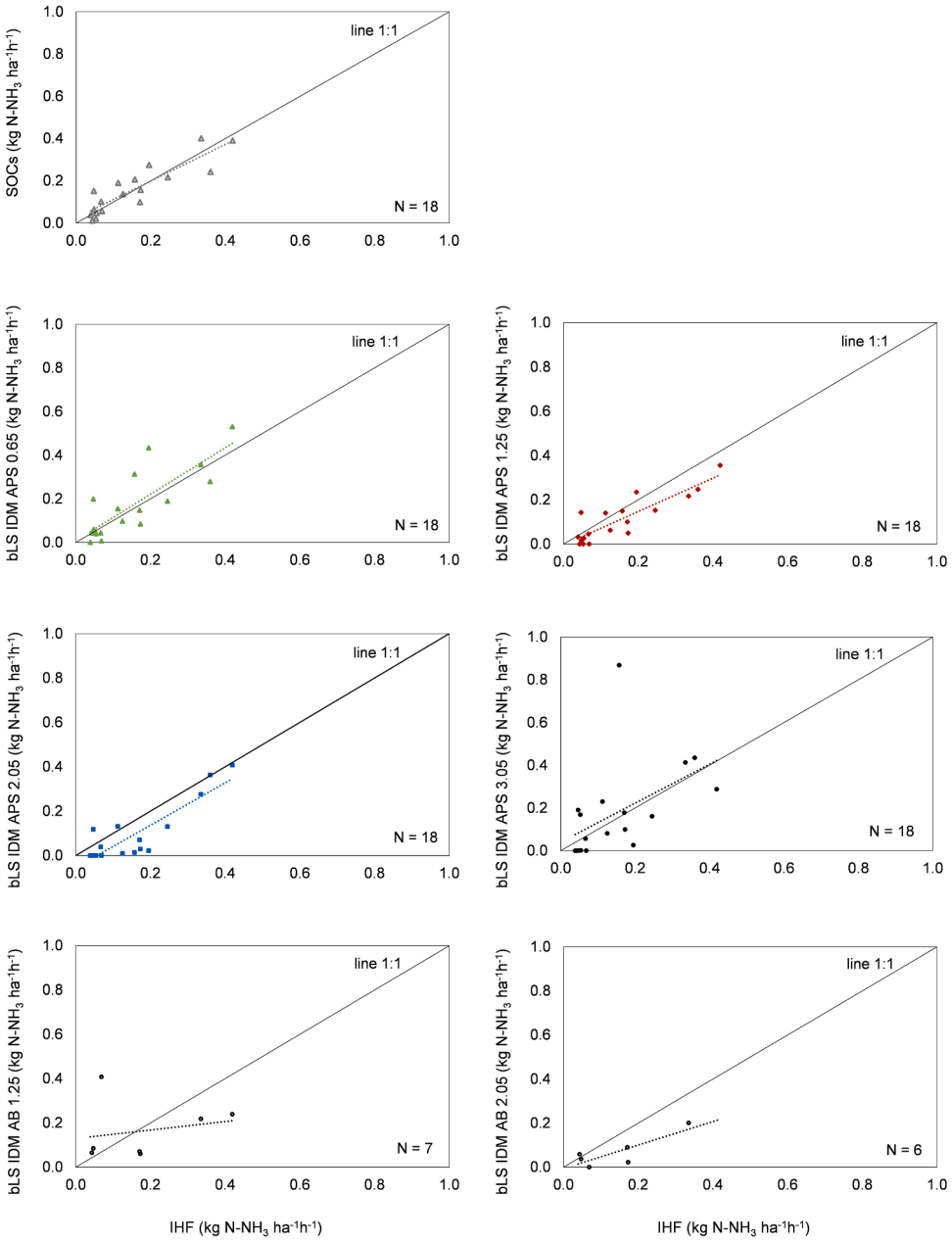

Fig. 4. IHF-obtained NH_3 emission fluxes and estimates from semiopen passive chambers (SOCs) and a backward Lagrangian stochastic inverse dispersion model (bLs IDM) combined with ALPHA® samplers (APSs) at heights of 0.65, 1.25, 2.05 and 3.05 m and with acid bubblers (ABs) at heights of 1.25 and 2.05 m.

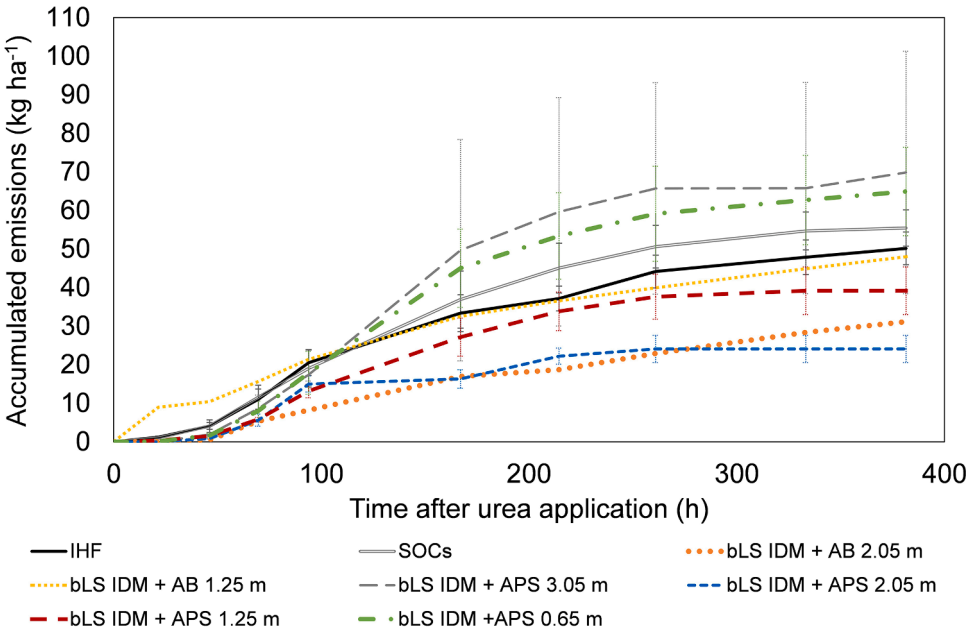

Fig. 5. Average IHF-obtained NH_3 cumulative emissions and estimates obtained using semiopen passive chambers and a backward Lagrangian stochastic inverse dispersion model combined with ALPHA® samplers (bLS IDM + APSs) at heights of 0.65, 1.25, 2.05 and 3.05 m and with acid bubblers (bLS IDM + AB) at heights of 1.25 and 2.05 m during the experimental period (the bars denote standard errors).

Table 3
IHF-based cumulative NH_3 emissions and estimates obtained using semiopen passive chambers and a backward Lagrangian stochastic inverse dispersion model combined with ALPHA® samplers (APSs) at heights of 0.65, 1.25, 2.05 and 3.05 m and with acid bubblers (ABs) at heights of 1.25 and 2.05 m, observed 381 h (16 days) after urea spreading. The emission rate (R) was calculated as kg N-NH_3 emitted/kg N applied.

	Cumulative emissions (E) after 16 days		Emission rate (R) (%)	Relative emissions E/E_{IHF}
	kg ha^{-1}	SE		
IHF	50.15	4.25	27.3%	
APS 0.65	64.90	11.46	35.3%	1.3
APS 1.25	39.17	6.17	21.3%	0.8
APS 2.05	24.08	3.51	13.1%	0.5
APS 3.05	69.82	31.44	37.9%	1.4
AB 1.25	47.99		26.1%	1.0
AB 2.05	31.15		16.9%	0.6
SOCs	55.44	4.70	30.1%	1.1

both with APSs and ABs, obtained the closest estimates to the IHF-based cumulative emissions (Fig. 5). The relative emissions (E/E_{IHF}) for these methods were the closest to unity, 0.8 for APSs, 1.0 for ABs and 1.1 for SOCs (Table 3). The bLS IDM method with APSs at 0.65 m overestimated the cumulative emissions by 29% (relative emission of 1.4).

4. Discussion

4.1. NH_3 daily fluxes and cumulative emissions

The emission peak appeared at the 70-94 HAUA sampling period; an average value of 0.34 kg N-NH_3 ha^{-1} h^{-1} (±0.02 S.E.) was reached. This result is consistent with other studies carried out under semi-arid conditions (e.g., Sanz et al., 2008; Scotto di Perta et al., 2019). However, emission rates from this single experimental campaign cannot be extended to any other conditions. The high humidity conditions and warm temperatures during the first 72 HAUA boosted urea hydrolysis, raising initial ammonium concentration values in the topsoil (0-10 cm) up to 106.56 (±34.79 S.E.) and 87.4 (±26.40 S.E.) kg N-NH_4^+ ha^{-1} in P1 and P2, respectively (Table S1). These values then decreased over the next 48 h to a minimum of 45.98 (±29.96 S.E.) in P1 and 46.45 (±19.61 S.E.) kg N-NH_4^+ ha^{-1} in P2, coinciding with the ammonia emission peak.

The temporal evolution of the NH_3 fluxes seen in all measuring methods was similar to that of the IHF-based values. However, the bLS IDM showed scattered estimates during the 5th sampling period, 94 to 167 HAUA. During this time, the estimates were probably affected by the drastic changes in the weather conditions observed. The effect of wind on NH_3 volatilization is well known (e.g., Denmead, 1983). Increasing wind conditions in our study (Fig. 2) may have boosted emitting fluxes in the 4th sampling period (Fig. 3).

The rainfall event (3.23 mm) at 139 HAUA likely favored the diffusion of NH_4^+ below the upper soil layer, thus lowering its pool and, therefore, abating the NH_3 emission rates, as observed 28 h later (167 HAUA). Although some authors consider that larger precipitation events (≥ 12 mm) are needed to detect this effect (Sanz-Cobena et al., 2011; Jones et al., 2013; Shigaki and Dell, 2015), our results were consistent with observations obtained in previous field experiments (Abalos et al., 2012; Martins et al., 2017).

The percentage of N-NH_3 emitted in relation to the N applied (27.3%), measured in this study with the IHF method, was in line with the results of previous studies using urea surface applied on bare or prairie soils (Martins et al., 2017; Recio et al., 2020; Soares et al., 2012; Sommer et al., 2005; UNECE, 2015). The values reported by the measuring methods ranged from 16.9% to 35.3%. In all cases, the obtained ammonia volatilization % was higher than those reported by Abalos et al. (2012) and Sanz-Cobena et al. (2008) under semi-arid conditions of Central Spain (6.7 and 10.1%, respectively), as well as the 14.2% urea NH_3 emission factors reported in the 2019 refinement of the 2006 IPCC accounting methodology (IPCC, 2019) and the 13.8% shown in the EMEP/EEA Air Pollutant Inventory Guidebook 2019 (Hutchings et al., 2019) for temperate climates (15-25°C) and high pH soils (>7.0). The measurements from the bLS IDM with samplers (ABs and APSs) placed at a height of 1.25 m showed the closest cumulative emission values to those obtained using the IHF method (Table 3).

4.2. Assessment of methods of NH_3 emission determination

4.2.1. Semiopen passive chambers

This field experiment was, to our knowledge, the first attempt to compare SOCs (designed according to Araújo et al. (2009) against micrometeorological methods (IHF and bLS dispersion models). SOCs, which are already proven to be accurate in tropical or humid continental climates, are simpler to use and less expensive (Martins et al., 2017; Shigaki and Dell, 2015). This method allows the easy deployment of replicates, as the labor demand is low; however, the method is limited by its low spatial representativeness (Sintermann et al., 2012), which intensifies when the soil surface undergoes any alteration; for example, N fertilizer incorporation likely increases flux heterogeneity (Ni et al., 2015) and in cropped fields the canopy effect cannot be considered. Even so, the result obtained in this study of the emission of 30.1% of the applied N was in accordance with the results of other studies using this methodology in shorter monitoring periods and with similar fertilization rates (Araújo et al., 2009; Mateo-Marín et al., 2021). This method is quite sensitive to the recovery efficiency factor and likely requires specific calibration for every experimental condition. Nevertheless, the significance of the linear regression with a high coefficient of determination (R^2=0.784) and no significant difference in the 1:1 line (slope 0.870; intercept 0.025) evidenced that SOCs can measure satisfactorily different emission rates (Table 2). In addition, the highest NSE and E1 indexes among all methods indicate minor differences with the reference IHF method, as well as the absence of extreme values. SOCs were robust and suitable for comparing treatments in accordance with Shigaki and Dell (2015) at affordable costs and work demands (Supplementary material, Table S5).

4.2.2. Alpha passive samplers with inverse dispersion model

In the concentration range of 3 to 260 μg NH_3 m^{-3}, the APSs showed no saturation when comparing emission fluxes with the IHF observations. However, for periods with low emission rates (<0.07 kg N-NH_3 h^{-1} ha^{-1}), a clear underestimation of the emission fluxes was provided by the APSs (Fig. 4). Moreover, the coefficients of variation (CVs) of NH_3 captured by the three replicates were larger in these periods of low emissions (Supplementary material, Fig. S1). This behavior arose when smaller amounts of NH_3 were captured by an APS, i.e., during low air NH_3 concentrations or for short exposure periods, and persisted independently of the wind speed, which was very low in the first samplings and higher in later periods (Fig. 2). The coefficients of variation at lower heights: 1.25 (14.5%) and 0.65 m (14.2%) were consistent with the results of Misselbrook et al. (2005), who found 13.9% variation in similar samplers. In our study, the precision of the PFSs used in the IHF method was not assessed. The horizontal flux density values were measured with only one PFS per height to infer every plot profile, which may counteract the precision of the method. However, Misselbrook et al. (2005) also tested PFS CV under controlled conditions using duplicates with similar results to APSs (10% vs 14%, respectively).

During the first and last sampling periods, the average NH_3 air concentrations measured in the two masts with APSs were similar to those measured in the background masts, leading to the determination of low or no emissions. In contrast, the PFSs, SOCs and ABs estimations in the last period showed higher sensitivity in detecting emissions at lower emission rates (Fig. 3).

Misselbrook et al. (2005) concluded that IHF mass balance is preferred for absolute emissions using passive flux samplers instead of independent concentration and wind speed measurements. Otherwise, direct measurement with APSs and ABs of the mean NH_3 air concentration avoids the systemic error incurred in other studies due to the unknown turbulent backflow component and is well suited to direct WindTrax input parameters. Additionally, they are free from empirical errors due to stall or bad alignment of the PFSs under low-wind conditions (Laubach et al., 2012). Leuning et al. (1985) established the threshold as 0.8 m s^{-1}. In this study, only the first 2 sampling periods had average wind speeds close to this limit (0.7 and 0.6 m s^{-1}, respectively), and in both cases, there was a prevailing wind direction during the whole interval (from N to S) (Fig. 2). For that reason, we believe that this condition did not affect the experimental results. APSs also represent a lower cost option with less labor demand in the laboratory (Supplementary material, Table S5). Some studies using the bLS IDM, which parametrized atmospheric turbulence, implemented filtering criteria for NH_3 observations under low wind speeds (friction velocity below 0.15 - 0.20 m s^{-1}) and extremely stable conditions according to the Monin-Obukhov stability theory (Carozzi et al., 2013a; Flesch et al., 2007, 2004; Shonkwiler and Ham, 2018; Wilson et al., 2012). Under these conditions, estimates may be inaccurate and should be excluded. Although badge-type samplers, such as APSs, are also sensitive to wind speed (Tang et al., 2001), this study simplifies calculations assuming neutral atmospheric stability (Ni et al., 2015; Sanz et al., 2010; Sommer et al., 2005) and no data were discarded. This contrasted with previous studies where data filtering due to weather conditions affected more than 40% of valuable data (Flesch et al., 2014; Shonkwiler and Ham, 2018).

The cumulative emissions observed at the different sampler heights, when tested compared to the IHF results (E/E_{IHF}, Table 3), revealed the strong influence of this parameter on the NH_3 flux determinations. A clear estimation pattern of higher NH_3 emissions at lower positions was detected in the two plots (Supplementary material, Table S3). This study shows that emission determination using ammonia concentrations measured below the optimum height leads to flux overestimations and that those measured at higher positions cause underestimation and inaccuracies, aligning with conclusions stated in other works, such as Yang et al. (2019).

The rainfall and a drastic increase in wind speed 139 h after urea spreading may have triggered the discrepancy among the flux estimates at the different heights for the 94-167 HAUA period. Only fluxes estimated at 1.25 and 0.65 m maintained the expected emission trend over time according to the overall pattern (Fig. 3). Periods of rapid atmospheric changes may affect both sampler performances, e.g., altering diffusivity parameters that drive APS operation and weakening the neutral stability assumptions adopted in the dispersion model (Wilson et al., 2012). The use of a long-term monitoring period may make the method more vulnerable to these circumstances (Fig. 3b).

The linear regression analysis indicated that the flux estimates obtained at 0.65, 1.25, and 2.05 m were strongly related to the IHF values, as opposed to those observed at 3.05 m, which presented a nonsignificant relation with the results of the IHF method. The slopes at 0.65 m (1.066) and 2.05 m (0.955) were the closest to 1 (Table 2) among all heights. The three lower heights showed slight differences between the estimates and IHF values according to rRMSE, NSE, and E1. Nevertheless, the 0.65 m position led to an overestimation of total emissions after 16 days (Table 3, E/E_{IHF} = 1.3) compared to the IHF results. The emissions derived at 1.25 m stayed closer (E/E_{IHF} = 0.8) and had a better relationship with the IHF fluxes. The results suggested that a sampling height of 1.25 m is the option that provides closer results to the IHF under these experimental conditions and may be considered for future research. This result is also in line with the conclusions presented by Sommer et al. (2005), who set the convenient height near 1.0 m in colder conditions for a short canopy with a similar experimental layout.

4.2.3. Acid bubblers with inverse dispersion models

The pattern of variation in ammonia fluxes depending on the height of APSs and the bLS IDM model was also observed with AB samplers; larger emission fluxes were estimated at the lower height. Nevertheless, the missing data at the 4th sampling at the 2.05-m height, coinciding with the emission peak, may have boosted the differences in cumulative emissions, which were 35% inferior to those at the height of 1.25 m (Table 3). In contrast, the unusually high observation at the 1.25-m height at the first sampling time did not cause an overestimation of cumulative flux estimates; If this time is omitted and interpolated, the

total emission measured at this position would be 39.7 kg N-NH_3, very close to the result obtained with an APS at 1.25 m (Table 3).

The linear regression analysis showed worse correlations of ABs with the IHF fluxes than in the case of APSs; the AB results are dominated by the effect of extreme values, as evidenced in the rRMSE index and the improvement in the E1 index in relation to the NSE at the 1.25-m height (Table 2).

The statistical analysis was strongly affected by only one replicate and the two sampling periods without measurements. This method obtained reasonably good estimates after the anomalies were discarded, although the accuracy and correlation were not as good as those observed for the other tested alternatives. In addition, ABs are an efficient monitoring system for NH_3 air concentration, but they are labor demanding and require a power supply and accurate control of the monitoring instrumentation to avoid anomalies (Supplementary material, Table S5).

4.3. Limitations of this research

The experimental design of this work faced some shortcomings. The plot surface and material requirements enabled 2 replicates separated by 50 m, P1 and P2, to ensure identical experimental conditions in the same field and sufficient separation. This experimental design has been accepted by the scientific community, and several studies have used two replicates (Carozzi et al., 2013b; Recio et al., 2020), or even only one plot, under similar conditions (Sommer et al., 2005; Yang et al., 2019). Besides, larger distances between plots would have ensured the absence of any cross contamination. However, according to previous studies, 50 m is sufficient, (e.g. Abalos et al., 2012; Recio et al., 2020; Sanz-Cobena et al., 2019, 2008) and the focus of this study was on method comparison, not on the accurate ammonia emission rate determination.

In addition, the results belong to a single experimental campaign. A direct shortcoming of this approach is that conclusions about emissions and the method's performance cannot be extended to any agronomic or climatic conditions as they belong to one single monitoring campaign. Nevertheless, the evolution of the NH_3 emissions throughout the experiment enabled us to assess the sensitivity and accuracy of 13 measures (7 in P1 and 5 in P2) performed with different methods against the IHF in each of the 9 long-term sampling intervals. They were under different weather conditions and NH_3 emission rates, ranging from values below the sampler detection limit up to 0.868 kg N-NH_3 ha^{-1} h^{-1}.

The duration of the measuring campaign (16 days) was decided to ensure accordance or an even larger experimental period than other method comparison works addressing NH_3 emission measurements after urea surface fertilization (Ni et al., 2015; Pacholski et al., 2006; Scotto di Perta et al., 2019; Shigaki and Dell, 2015; Sommer et al., 2005; Turner et al., 2010). Emission peaks under these circumstances usually appear within the first 48-72 hours (Pacholski et al., 2006; Scotto di Perta et al., 2019; Sommer et al., 2005).

The use of urea surface application on bare soil as an NH_3 emitting source prevents the analysis of the canopy effect on the method's variability. This design decision was made to reduce the number of variables affecting the measurement, and it was made according to the common agricultural practice of N fertilizer application as a base dressing and in agreement with other studies (Sanz-Cobena et al., 2011, 2008; Scotto di Perta et al., 2019; Turner et al., 2010).

Finally, the installation of several sensing systems simultaneously in the experimental field may produce interferences with each other and alter the accuracy of the measured values. For that reason, no bulky instruments were used, and all the devices were carefully installed, minimizing any crossed effect (Supplementary material, picture compilation). The use of triplicate PFSs per height would have provided better information about the samplers' precision. However, they may have been subjected to the abovementioned experimental interference.

Despite the limitations mentioned above, the consistency of the emission fluxes observed with other studies (Section 4.1) allows us to conclude that the experiment was performed under enough representative agricultural conditions to contribute valuable information to the method comparison.

5. Conclusions

Our results suggested that SOCs are a robust tool that can be used for qualitative assessments when comparing treatments. They offer the possibility of making unbiased replications using small areas. The backwards Lagrangian stochastic IDM combined with time-averaged concentration samplers at a 1.25-m height gave the closest cumulative emission estimations to the IHF. Sampler data from positions 2.05- and 3.05-m heights should be discarded due to a lack of accuracy of the sampling methods used at low NH_3 exposure rates and the influence of weather conditions on the precision of the estimations, in addition to their underestimation trend. Accordingly, overestimation was evidenced at the lower position. An incorrect decision in the setup of monitoring heights combined with unexpected weather changes may considerably compromise ammonia emission estimates.

The use of the bLS IDM with extended sampling intervals (from 22 to 73 h) (assuming a continuous neutral stability approach) of air ammonia concentration with APSs at 1.25 m manifested little divergence in the obtained flux estimates with the mass balance IHF values. It should be considered that this study demonstrated that the bLS IDM + APS is a low-sensitivity method under low emission rates (below 0.07 kg N ha^{-1} h^{-1}). Our results supported this method, as well as SOCs, as cost-efficient alternatives for simple on-site monitoring.

Declaration of Competing Interest

The authors declare that they have no known competing financial interests or personal relationships that could have appeared to influence the work reported in this paper.

Acknowledgment

This work was supported by the LIFE Programme with European Union funds under the LIFE ARIMEDA project (LIFE16 ENV/ES/000400). The authors of this work would like to thank to the field and laboratory personnel of the CITA's Department of Soil and Irrigation, to the Autonomous Community of Madrid and Universidad Politécnica de Madrid for their support with the project APOYO-JOVENES-NFW8ZQ-42-XE8B5K and to the Coordinated Research Project (No. CRP D15020) of the Soil and Water Management and Crop Nutrition Section, Joint FAO/IAEA Division of Nuclear Techniques in Food and Agriculture, through the Technical Contract "Development, Validation and Refining of New Ammonia Emission Method on Field Scale Using Nuclear" (No. 24236) .

Supplementary materials

Supplementary material associated with this article can be found, in the online version, at doi:10.1016/j.agrformet.2021.108517.

References

Abalos, D., Sanz-Cobena, A., Misselbrook, T., Vallejo, A., 2012. Effectiveness of urease inhibition on the abatement of ammonia, nitrous oxide and nitric oxide emissions in a non-irrigated Mediterranean barley field. Chemosphere 89, 310–318. https://doi.org/10.1016/j.chemosphere.2012.04.043.

Araújo, E.da S., Marsola, T., Miyazawa, M., Soares, L.H.de B., Urquiaga, S., Boddey, R.M., Alves, B.J.R., 2009. Calibration of a semi-opened static chamber for the quantification of volatilized ammonia from soil. Pesqui. Agropecu. Bras. 44, 769–776. https://doi.org/10.1590/S0100-204×2009000700018.

Carozzi, M., Ferrara, R.M., Rana, G., Acutis, M., 2013a. Evaluation of mitigation strategies to reduce ammonia losses from slurry fertilisation on arable lands. Sci. Total Environ. 449, 126–133. https://doi.org/10.1016/j.scitotenv.2012.12.082.

Carozzi, M., Loubet, B., Acutis, M., Rana, G., Ferrara, R.M., 2013b. Inverse dispersion modelling highlights the efficiency of slurry injection to reduce ammonia losses by agriculture in the Po Valley (Italy). Agric. For. Meteorol. 171–172, 306–318. https://doi.org/10.1016/j.agrformet.2012.12.012.

Denmead, O.T., 1983. Gaseous loss of nitrogen from plant-soil systems. Development in Plant and Soil Sciences. Springer-Science+Business Media, B.V. https://doi.org/10.1017/CBO9781107415324.004

European Environmental Agency, 2019. European Environmental Agency. (2019). Air quality in Europe — 2019 report — EEA Report No 10/2019 (Issue 10). https://doi.org/10.2800/822355Air quality in Europe — 2019 report — EEA Report No 10/2019. https://doi.org/10.2800/02825.

Flesch, T.K., McGinn, S.M., Chen, D., Wilson, J.D., Desjardins, R.L., 2014. Data filtering for inverse dispersion emission calculations. Agric. For. Meteorol. 198–199, 1–6. https://doi.org/10.1016/j.agrformet.2014.07.010.

Flesch, T.K., Wilson, J.D., Harper, L.A., Crenna, B.P., Sharpe, R.R., 2004. Deducing ground-to-air emissions from observed trace gas concentrations: a field trial. J. Appl. Meteorol. 43, 487–502. https://doi.org/10.1175/JAM2214.1.

Flesch, T.K., Wilson, J.D., Harper, L.A., Todd, R.W., Cole, N.A., 2007. Determining ammonia emissions from a cattle feedlot with an inverse dispersion technique. Agric. For. Meteorol. 144, 139–155. https://doi.org/10.1016/j.agrformet.2007.02.006.

Häni, C., Sintermann, J., Kupper, T., Jocher, M., Neftel, A., 2016. Ammonia emission after slurry application to grassland in Switzerland. Atmos. Environ. 125, 92–99. https://doi.org/10.1016/j.atmosenv.2015.10.069.

Hutchings, N., Webb, J., Amon, B., 2019. EMEP/EEA air pollutant emission inventory guidebook 2019. Build. Robot. LEGO Mindstorms NXT 3.D Crop P. https://doi.org/10.1016/b978-159749152-5/50001-2.

Insausti, M., Timmis, R., Kinnersley, R., Rufino, M.C., 2020. Advances in sensing ammonia from agricultural sources. Sci. Total Environ. 706, 135124 https://doi.org/10.1016/j.scitotenv.2019.135124.

IPCC 2019, 2019. In: Calvo Buendia, E., Tanabe, K., Kranjc, A., Baasansuren, J., Fukuda, M., Ngarize, S., Osako, A., Pyrozhenko, Y., Shermanau, P., Federici, S. (Eds.), Refinement to the 2006 IPCC Guidelines for National Greenhouse Gas Inventories. Published: IPCC, Switzerland.

Jantalia, C.P., Halvorson, A.D., Follett, R.F., Alves, B.J.R., Polidoro, J.C., Urquiaga, S., 2012. Nitrogen source effects on ammonia volatilization as measured with semi-static chambers. Agron. J. 104, 1595–1603. https://doi.org/10.2134/agronj2012.0210.

Jones, C., Brown, B.D., Engel, R., Horneck, D., Olson-Rutz, K., 2013. Nitrogen Fertilizer Volatilization. Montana State University Extension. https://landresources.montana.edu/soilfertility/documents/PDF/pub/UvolfactEB0208.pdf. Accessed: 25th May 2021.

Laubach, J., Taghizadeh-Toosi, A., Sherlock, R.R., Kelliher, F.M., 2012. Measuring and modelling ammonia emissions from a regular pattern of cattle urine patches. Agric. For. Meteorol. 156, 1–17. https://doi.org/10.1016/j.agrformet.2011.12.007.

Leuning, R., Freney, J.R., Denmead, O.T., Simpson, J.R., 1985. A sampler for measuring atmospheric ammonia flux. Atmos. Environ. 19, 1117–1124. https://doi.org/10.1016/0004-6981(85)90196-9.

Lorenzo-Gonzalez, M.A., Quilez, D., Isidoro, D., 2013. Statistical behavior of monthly load estimators. Trans. ASABE 56, 1387–1396. https://doi.org/10.13031/trans.56.9965.

Loubet, B., Carozzi, M., Voylokov, P., Cohan, J.P., Trochard, R., Génermont, S., 2018. Evaluation of a new inference method for estimating ammonia volatilisation from multiple agronomic plots. Biogeosciences 15, 3439–3460. https://doi.org/10.5194/bg-15-3439-2018.

Loubet, B., Génermont, S., Ferrara, R., Bedos, C., Decuq, C., Personne, E., Fanucci, O., Durand, B., Rana, G., Cellier, P., 2010. An inverse model to estimate ammonia emissions from fields. Eur. J. Soil Sci. 61, 793–805. https://doi.org/10.1111/j.1365-2389.2010.01268.x.

Martins, M.R., Sant'Anna, S.A.C., Zaman, M., Santos, R.C., Monteiro, R.C., Alves, B.J.R., Jantalia, C.P., Boddey, R.M., Urquiaga, S., 2017. Strategies for the use of urease and nitrification inhibitors with urea: impact on N_2O and NH_3 emissions, fertilizer-15N recovery and maize yield in a tropical soil. Agric. Ecosyst. Environ. 247, 54–62. https://doi.org/10.1016/j.agee.2017.06.021.

Martins, M.R., Sarkis, L.F., Guareschi, R.F., Santos, C.A., Sant'anna, S.A.C., Zaman, M., Jantalia, C.P., Alves, B.J.R., Boddey, R.M., Araújo, E.S., Urquiaga, S., 2021. A simple and easy method to measure ammonia volatilization: accuracy under field conditions. Pedosphere 31, 255–264. https://doi.org/10.1016/S1002-0160(20)60077-7.

Mateo-Marín, N., Isla, R., Quílez, D., 2021. Gaseous nitrogen losses from pig slurry fertilisation: can they be reduced with additives in a wheat crop. Span. J. Agric. Res. *In press*.

Misselbrook, T.H., Nicholson, F.A., Chambers, B.J., Johnson, R.A., 2005. Measuring ammonia emissions from land applied manure: an intercomparison of commonly used samplers and techniques. Environ. Pollut. 135, 389–397. https://doi.org/10.1016/j.envpol.2004.11.012.

Ni, K., Köster, J.R., Seidel, A., Pacholski, A., 2015. Field measurement of ammonia emissions after nitrogen fertilization-A comparison between micrometeorological and chamber methods. Eur. J. Agron. 71, 115–122. https://doi.org/10.1016/j.eja.2015.09.004.

Pacholski, A., Cai, G., Nieder, R., Richter, J., Fan, X., Zhu, Z., Roelcke, M., 2006. Calibration of a simple method for determining ammonia volatilization in the field - Comparative measurements in Henan Province. China. Nutr. Cycl. Agroecosyst. 74, 259–273. https://doi.org/10.1007/s10705-006-9003-4.

Pedersen, J.M., Feilberg, A., Kamp, J.N., Hafner, S., Nyord, T., 2020. Ammonia emission measurement with an online wind tunnel system for evaluation of manure application techniques. Atmos. Environ. 230, 117562 https://doi.org/10.1016/j.atmosenv.2020.117562.

Perazzolo, F., Mattachini, G., Tambone, F., Misselbrook, T., Provolo, G., 2015. Effect of mechanical separation on emissions during storage of two anaerobically codigested animal slurries. Agric. Ecosyst. Environ. 207, 1–9. https://doi.org/10.1016/j.agee.2015.03.023.

Puchalski, M.A., Sather, M.E., Walker, J.T., Lehmann, C.M.B., Gay, D.A., Mathew, J., Robarge, W.P., 2011. Passive ammonia monitoring in the United States: Comparing three different sampling devices. J. Environ. Monit. 13, 3156–3167. https://doi.org/10.1039/c1em10553a.

Recio, J., Montoya, M., Ginés, C., Sanz-Cobena, A., Vallejo, A., Alvarez, J.M., 2020. Joint mitigation of NH_3 and N_2O emissions by using two synthetic inhibitors in an irrigated cropping soil. Geoderma 373, 114423. https://doi.org/10.1016/j.geoderma.2020.114423.

Sanz-Cobena, A., Lassaletta, L., Estellés, F., Del Prado, A., Guardia, G., Abalos, D., Aguilera, E., Pardo, G., Vallejo, A., Sutton, M.A., Garnier, J., Billen, G., 2014. Yield-scaled mitigation of ammonia emission from N fertilization: the Spanish case. Environ. Res. Lett. 9 https://doi.org/10.1088/1748-9326/9/12/125005.

Sanz-Cobena, A., Misselbrook, T., Camp, V., Vallejo, A., 2011. Effect of water addition and the urease inhibitor NBPT on the abatement of ammonia emission from surface applied urea. Atmos. Environ. 45, 1517–1524. https://doi.org/10.1016/j.atmosenv.2010.12.051.

Sanz-Cobena, A., Misselbrook, T.H., Arce, A., Mingot, J.I., Diez, J.A., Vallejo, A., 2008. An inhibitor of urease activity effectively reduces ammonia emissions from soil treated with urea under Mediterranean conditions. Agric. Ecosyst. Environ. 126, 243–249. https://doi.org/10.1016/j.agee.2008.02.001.

Sanz-Cobena, A., Misselbrook, T.H., Hernáiz, P., Vallejo, A., 2019. Impact of rainfall to the effectiveness of pig slurry shallow injection method for NH_3 mitigation in a Mediterranean soil. Atmos. Environ. 216, 116913 https://doi.org/10.1016/j.atmosenv.2019.116913.

Sanz, A., Misselbrook, T., Sanz, M.J., Vallejo, A., 2010. Use of an inverse dispersion technique for estimating ammonia emission from surface-applied slurry. Atmos. Environ. 44, 999–1002. https://doi.org/10.1016/j.atmosenv.2009.08.044.

Scotto di Perta, E., Fiorentino, N., Gioia, L., Cervelli, E., Faugno, S., Pindozzi, S., 2019. Prolonged sampling time increases correlation between wind tunnel and integrated horizontal flux method. Agric. For. Meteorol. 265, 48–55. https://doi.org/10.1016/j.agrformet.2018.11.005.

Searle, P.L., 1984. The berthelot or indophenol reaction and its use in the analytical chemistry of nitrogen: a review. Analyst 109, 549–568. https://doi.org/10.1039/AN9840900549.

Shah, S.B., Westerman, P.W., Arogo, J., 2006. Measuring ammonia concentrations and emissions from agricultural land and liquid surfaces: a review. J. Air Waste Manag. Assoc. 56, 945–960. https://doi.org/10.1080/10473289.2006.10464512.

Shigaki, F., Dell, C.J., 2015. Comparison of low-cost methods for measuring ammonia volatilization. Agron. J. 107, 1392–1400. https://doi.org/10.2134/agronj14.0431.

Shonkwiler, K.B., Ham, J.M., 2018. Ammonia emissions from a beef feedlot: Comparison of inverse modeling techniques using long-path and point measurements of fenceline NH_3. Agric. For. Meteorol. 258, 29–42. https://doi.org/10.1016/j.agrformet.2017.10.031.

Sintermann, J., Neftel, A., Ammann, C., Häni, C., Hensen, A., Loubet, B., Flechard, C.R., 2012. Are ammonia emissions from field-applied slurry substantially over-estimated in European emission inventories? Biogeosciences 9, 1611–1632. https://doi.org/10.5194/bg-9-1611-2012.

Soares, J.R., Cantarella, H., Menegale, M.L., de, C., 2012. Ammonia volatilization losses from surface-applied urea with urease and nitrification inhibitors. Soil Biol. Biochem. 52, 82–89. https://doi.org/10.1016/j.soilbio.2012.04.019.

Sommer, S.G., McGinn, S.M., Flesch, T.K., 2005. Simple use of the backwards Lagrangian stochastic dispersion technique for measuring ammonia emission from small field-plots. Eur. J. Agron. 23, 1–7. https://doi.org/10.1016/j.eja.2004.09.001.

Tang, Y.S., Cape, J.N., Sutton, M.A., 2001. Development and types of passive samplers for monitoring atmospheric NO_2 and NH_3 concentrations. ScientificWorldJournal 1, 513–529. https://doi.org/10.1100/tsw.2001.82.

Theobald, M.R., Sanz-Cobena, A., Vallejo, A., Sutton, M.A., 2015. Suitability and uncertainty of two models for the simulation of ammonia dispersion from a pig farm located in an area with frequent calm conditions. Atmos. Environ. 102, 167–175. https://doi.org/10.1016/j.atmosenv.2014.11.056.

Turner, D.A., Edis, R.B., Chen, D., Freney, J.R., Denmead, O.T., Christie, R., 2010. Determination and mitigation of ammonia loss from urea applied to winter wheat with N-(n-butyl) thiophosphorictriamide. Agric. Ecosyst. Environ. 137, 261–266. https://doi.org/10.1016/j.agee.2010.02.011.

UNECE, 2015. United Nations Economic Commission for Europe Framework Code for good agricultural practice for reducing ammonia emissions. Int. Organ. 14, 189–202. https://doi.org/10.1017/S0020818300001818.

UNEP, 2019. Frontiers 2018/19 Emerging Issues of Environmental Concern. United Nations Environment Programme, Nairobi. Front. 2018/19 Emerg. Issues Environ. Concern 52–62.

WHO, 2019. In: Diseases and Air Pollution WHO European High-Level Conference on Noncommunicable Diseases.

Wilson, J.D., Catchpoole, V.R., Denmead, O.T., Thurtell, G.W., 1983. Verification of a simple micrometeorological method for estimating the rate of gaseous mass transfer from the ground to the atmosphere. Agric. Meteorol. 29, 183–189.

Wilson, J.D., Flesch, T.K., Crenna, B.P., 2012. Estimating surface-air gas fluxes by inverse dispersion using a backward lagrangian stochastic trajectory model. Geophys. Monogr. Ser. 200, 149–161. https://doi.org/10.1029/2012GM001269.

Wilson, J.D., Thurtell, G.W., Kidd, G.E., Beauchamp, E.G., 1982. Estimation of the rate of gaseous mass transfer from a surface source plot to the atmosphere. Atmos. Environ. 16, 1861–1867. https://doi.org/10.1016/0004-6981(82)90374-2.

Yang, W., Que, H., Wang, S., Zhu, A., Zhang, Y., He, Y., Xin, X., Zhang, X., 2019. Comparison of backward Lagrangian stochastic model with micrometeorological mass balance method for measuring ammonia emissions from rice field. Atmos. Environ. 211, 268–273. https://doi.org/10.1016/j.atmosenv.2019.05.028.